Vol. 1(1), pp. 1-24, September 2022
DOI: xx.0001/AJPC2021.0207
ISSN 2021-xxxx

ASEAN Journal of Process Control

Research Article

Plantwide Design and Control of Sulfur-Iodine Thermochemical Cycle Plant for Hydrogen Production

Noraini Mohd[1*], Jobrun Nandong[2]

[1] School of Energy and Chemical Engineering, Xiamen University Malaysia, 43900 Sepang, Selangor Darul Ehsan, MALAYSIA

[2] Department of Chemical Engineering, Curtin University Malaysia, Miri 98009, Sarawak, MALAYSIA

*Corresponding Author: noraini.mohd@xmu.edu.my

Academic Editor: Yudi Samyudia
Received: 29 November 2021; Accepted: 15 July 2022; Published: 1 September 2022

Abstract: Through several credible studies, some researchers have identified the Sulfur-Iodine Thermochemical Cycle (SITC) process as the most promising one among over 350 different types of thermochemical cycles for large-scale hydrogen production. Detailed complete design and control study of the SITC plant at an industrial scale so far remains scarce. This paper presents the plantwide design and control study based on a pre-defined SITC flowsheet. In the flowsheet, a multi-bayonet reactor configuration is adopted in the sulfuric acid decomposition section to improve the plant's thermal efficiency. A fundamental model of the complete SITC plant enables process scale-up, optimization, and plantwide simulation. The Self-Optimizing Control Structure (SOCS) approach is adopted to construct a complete control (PWC) strategy for the SITC plant. The plantwide SOCS strategy enables robust and flexible operation of the SITC plant, which allows the production rate to vary over a wide range, from 24 tons/day to 57.6 tons/day of hydrogen without leading to unstable operation. At the maximum production capacity, the plant's thermal efficiency reaches 68.6% and gross profit of USD 35 million per annum. The extensive simulation study shows that it is vital to control the Bunsen reactor well within a narrow range of conditions. Poor control of the Bunsen reactor can lead to severe challenges to achieving smooth plant operation overall. The proposed PWC strategy was able to provide sufficient control of SITC towards economic and controllability.

Keywords: Hydrogen Fuel; Thermochemical Cycle; Plantwide Control; Renewable Energy.

1. Introduction

Many scientists have recognized hydrogen as a promising alternative to fossil fuels partly because hydrogen combustion does not emit any greenhouse gas. However, the environmental impact of hydrogen production should be observed throughout its lifecycle, i.e., from raw material extraction to consumption which involves several stages. For this reason, the choices of technology and raw materials for hydrogen production should play a vital role in minimizing the overall environmental impact of the fuel - hence ensuring its sustainability. Therefore, for hydrogen production to be sustainable, the raw materials should be naturally abundant, such as water. One of the promising processes that can use

water as the raw material for hydrogen production is the so-called Sulfur-Iodine Thermochemical Cycle (SITC) process. Although the SITC technology is still immature, rapid developmental progress has been attained through intensive research worldwide.

Unlike the energy-intensive water hydrolysis process that uses electrical energy to split the water molecules into hydrogen and oxygen, a thermochemical cycle can split water molecules into hydrogen and oxygen directly using thermal energy [1]. In this regard, the thermal energy required for the thermochemical process might come from solar or waste heat of a high-temperature plant, e.g., from a nuclear reactor. Consequently, the thermochemical cycle process has the potential to reduce the cost of hydrogen production from water. Note that, to date, there are more than 350 thermochemical cycles identified and evaluated by the DOE-EERE Fuel Cell Technologies Program, Sandia National Laboratories, under a project called Solar Thermochemical Cycles for Hydrogen production (STCH) [2]. An extensive report by R.Perret (2011) [2] has pointed out several advantages of the SITC process - demonstrating experimental and technical feasibility, improved efficiency, and stability compared to other types of thermochemical cycles.

Extensive researches on the SITC process are available in the literature. In 2021, an integrity test on a SITC pilot plant scale made of practical structural materials and the stability of hydrogen production in harsh working conditions were carried out by N.Hiroki *et al* (2021) [3]. The team constructed a test facility from corrosion-resistant components that are developed using industrial materials. However, detailed studies on the design, optimization and control aspects of the process remain limited. To date, several important questions related to these three aspects are still open for more detailed analysis. The present paper articulates three questions about the SITC process. First, is the process viable on controllability and economic grounds? Second, which section poses the most difficult challenge to the operation and control? Third, how practical is the optimal plant-wide control strategy for the SITC plant? To answer the questions, a Plantwide Control (PWC) study on the complete SITC plant is performed. The main objective is to design a SITC plant flowsheet for a minimum production rate of 24 tonnes/day of hydrogen. The amount of hydrogen production rate chosen is the minimum production rate of an industrial-scale plant and is also comparable with that of the currently operational electrolysis industrial-scale plant [4][5]. The performed SITC design task includes (1) SITC flowsheet development, (2) the process scale-up from laboratory scale to industrial scale production and (3) PWC structure development. In addition, this work also introduces a new optimization technique called the Optimal-Practical Plantwide (OPPWIDE) for the PWC. This OPPWIDE method can determine an optimal control structure that gives the desired trade-off between economic performance and process controllability.

The PWC development for the SITC plant can pose a significant challenge, partly due to some unknown parameters such as the precise kinetics of the reaction mechanism at the pre-commercial scale stage and the lack of fundamental understanding of the process at an industrial scale. Because of the lack of existing knowledge in this uncharted territory, a set of PWC preliminary steps is proposed to gain some basic understanding of the problem before PWC design. The method presented by T.Larsson and S.Skogestad (2000) [6] called the Self-Optimizing Control Structure (SOCS) is used to design an optimal control strategy for the SITC plant. Note that the SOCS method consists of seven steps, divided into top-down and bottom-up parts where the goal is to find an optimal control structure of the given plant. The detailed PWC design in this work is based on the SOCS method. Bear in mind that a new industrial plant flowsheet is viable if it can simultaneously demonstrate acceptable economic and dynamic (controllability) performance indices where the failure to do so means that the plant is not feasible.

2. Process Design

2.1. Process Description

There are three main reactions in the SITC process with each reaction representing a section of the plant. Section I represents the Bunsen reaction which produces two key intermediates: hydrogen iodide (HI) and sulfuric acid (H_2SO_4). Section II covers the H_2SO_4 decomposition producing sulfur dioxide (SO_2) and O_2. Finally, Section III includes the HI decomposition to generate hydrogen (product). Equations (1) to (3) show the three overall chemical reactions mentioned above [7].

Section I: Exothermic Reaction, ΔH = -165 kJ/mol

$$I_2 + SO_2 + 2H_2O \rightleftharpoons H_2SO_4 + 2HI \quad (1)$$

Section II: Endothermic Reaction, ΔH = +371 kJ/mol

$$H_2SO_4 \rightleftharpoons H_2O + \frac{1}{2}O_2 + SO_2 \quad (2)$$

Section III: Endothermic Reaction, ΔH = +173 kJ/mol

$$2HI \rightleftharpoons H_2 + I_2 \quad (3)$$

Figure 1 shows the interconnections of the aforementioned three SITC sections. The water splitting is carried out via chemical reactions using SO_2 and I_2 that are recycled from Section II and Section III, respectively. To understand the operation of the process, it is important to investigate the key parameters affecting the process operation. The inlet and outlet variables of each section are listed in Table 1. There are at least ten input and output variables for each section of the SITC process. Each variable plays a significant role in determining the dynamic controllability of the SITC plant, and therefore, its nominal value needs to be optimized accordingly to meet the desired performance and production capacity.

At the plantwide level, several mechanisms and process interactions can determine the SITC dynamics and performance. One critical phenomenon affecting the efficiency of the SITC plant is the formation of different immiscible phases in the Bunsen reactor [8]. Bear in mind that the Bunsen Section is the heart of the SITC process - the reaction yield must be high enough to produce an effluence composition well above the azeotropic (H2O-I2-HI) composition. Meeting this objective in the Bunsen section is vital to enable the smooth operation of those other sections.

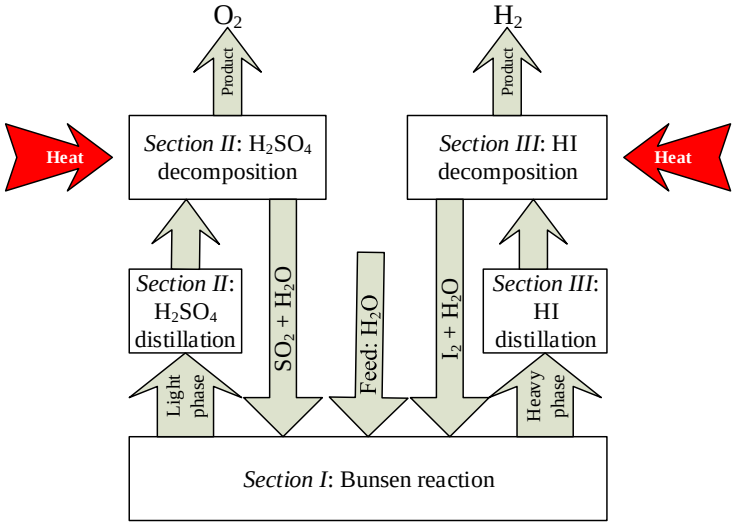

Figure 1. SITC process flow diagram with Section I, Section II and Section III [9]

Table 1: Input and output variables of the SITC process.

Section	Input	Output
I (Bunsen)	1. Feed iodine flow rate 2. Feed sulfur dioxide flow rate 3. Feed water and iodine mixture flow rate 4. Feed sulfur dioxide gas flow rate 5. Feed temperature 6. Feed cooling water temperature 7. Feed cooling water flow rate	1. Sulfuric acid flow rate 2. Hydrogen iodide flow rate 3. Trace of iodide concentration 4. Water flow rate 5. Trace of sulfur dioxide concentration 6. Outlet temperature 7. Outlet cooling water temperature
II (H_2SO_4)	1. Feed sulfuric acid flow rate 2. Feed sulfuric acid concentration 3. Feed temperature 4. Feed heating element temperature 5. Feed heating element flow rate	1. Oxygen flow rate 2. Outlet temperature 3. Sulfuric acid conversion 4. Sulfur dioxide flow rate 5. Sulfur trioxide flow rate

III (HI)	1. Feed hydrogen iodide concentration 2. Feed flow rate of hydrogen iodide 3. Feed temperature 4. Feed heating element temperature 5. Feed heating element flow rate	1. Hydrogen flow rate 2. Outlet reactor temperature 3. Hydrogen yield 4. Water/iodine flow rate 5. Hydrogen iodide flow rate

2.2. Process Flowsheet

Figure 2 depicts the process flow diagram of the proposed SITC flowsheet in this current work. The flowsheet is a modified version of the flowsheet in B.J. Lee (2009) [10]. The process starts in the Bunsen reactor (R-001) (Section I), in which I2, SO2, and H2O react to form sulfuric acid and hydrogen iodide. Due to excess water and iodine over sulfur dioxide in the feed, the reactor effluence containing unreacted water and iodine goes to a liquid-liquid (L-L) separator (V-001). The L-L separator functions based on two immiscible layers are formed that are spontaneous if the composition of the reactor effluence is above the $HI - H_2O - I_2$ (HIx) azeotropic composition. However, if the effluence composition is below the azeotropic composition, then the immiscible layers will not be formed spontaneously. Consequently, this will cause some problems in the operations of Sections II and III. Two streams are leaving the L-L separator: a light stream containing H_2SO_4 in water and a heavy stream containing HI in liquid iodine. The heavy layer is drawn from the bottom of the L-L separator while the light layer first overflows over the V-notch weir into the collecting compartment – the light stream is drawn from this compartment.

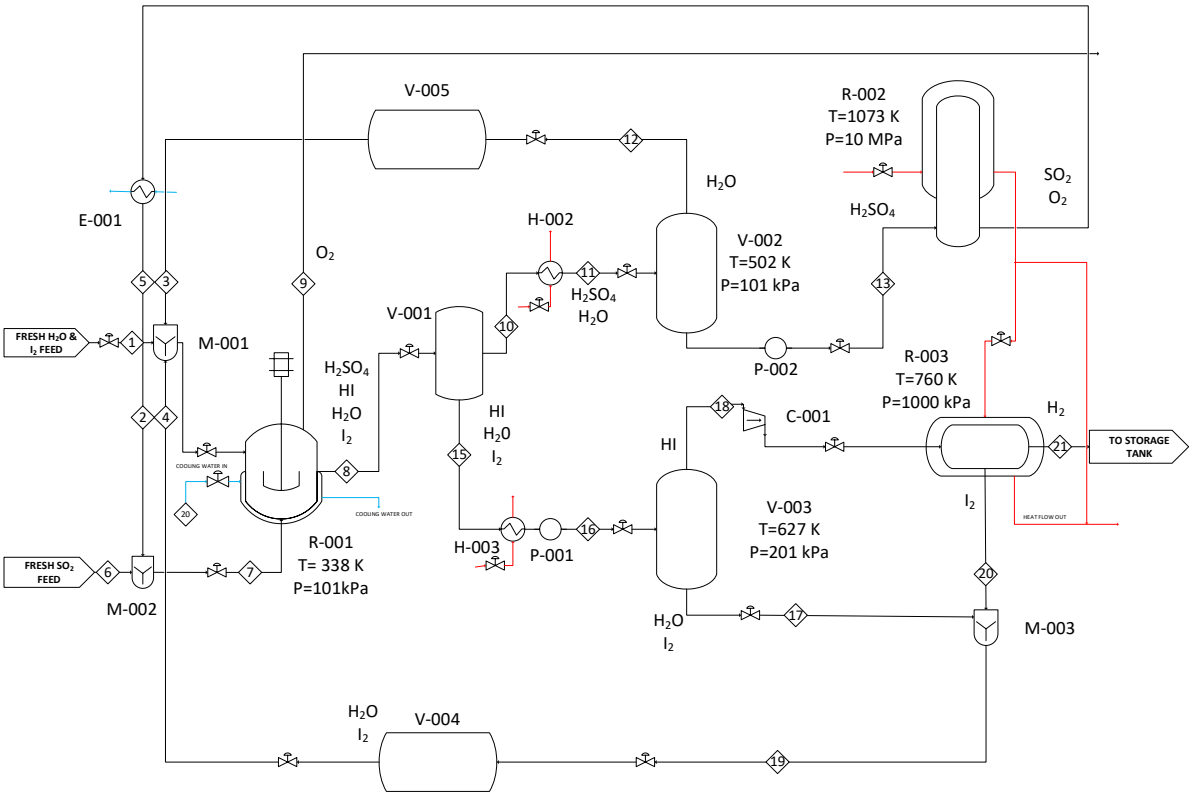

Figure 2. The pseudo-industrial-scale SITC plant process flow diagram

The light phase from the L-L separator is pre-heated before being fed into a flash tank (V-002) (Section II) where excess water is evaporated out. The concentrated sulfuric acid is subsequently sent to an integrated reactor namely, the Sulfuric Acid Integrated Boiler Superheater Decomposer (SA-IBSD) (R-002). The SA-IBSD reactor consists of multiple bayonet reactors arranged according to a shell-and-tube heat exchanger configuration. In the SA-IBSD reactor, the H_2SO_4 vapour is heated up to above 850°C before it is forced to flow through the catalyst bed. Hence, H_2SO_4 decomposition occurs converting the acid into sulfur dioxide (SO_2), water and oxygen. The product stream (containing both

SO_2 and O_2) from the SA-IBSD reactor is then cooled down before being recycled back to Section I. Meanwhile, the O_2 gas is drawn from the Bunsen reactor headspace and collected as a byproduct while the SO_2 gas dissolves into the liquid mixture inside the Bunsen reactor. Note that the SA-IBSD reactor used in this study is different from the decomposition reactor proposed by B. J. Lee *et al.* [10], which used two separate pieces of equipment to accomplish the sulfuric acid decomposition. Lee et al. (2009) [10] used a sulfuric acid evaporator and a sulfur trioxide (SO_3) decomposer to produce SO_2 and O_2.

The heavy (HI) stream from the L-L separator is pre-heated before being fed to another flash tank (V-003) located in Section III. The flash tank is heated to evaporate the excess water in the HI phase. The concentrated HI phase is then sent to a hydrogen iodide decomposer (HI-DE) unit (R-003). The HI-DE unit is a multi-tubular reactor in which suitable catalyst pellets are packed inside the tubes while a hot medium flows in the shell side. The heating source for the HI-DE unit comes from the excess heat available in the heating medium initially used in the SA-IBSD reactor. The hydrogen iodide decomposition occurs inside the tubes forming hydrogen and iodine. A mixture consisting of traces of HI, I_2, and H_2O is recycled back to Section I while hydrogen which is the main product is sent to a cryogenic liquid storage tank.

2.3. Design and Control Objectives

The PWC design for the SITC plant flowsheet shown in Figure 2 starts with defining the process control objectives. Two control objectives are specified for the given SITC plant as follows. The first objective is to achieve a minimum hydrogen production rate of 1 ton/hr (or 24 tons/day). The specified minimum hydrogen production rate is comparable with that of a currently operational electrolysis plant [5], and that of the Japan Atomic Energy Agency (JAEA) industrial-scale thermochemical cycle plant [4]. The second objective is to keep the molar feed flow of iodine to that of water (I_2/H_2O ratio) into the Bunsen Section at an optimum ratio. Lee et al. (2008) [11] proposed that an optimum operating range for I_2/H_2O molar feed flow ratio into the Bunsen reactor should be between 0.333 and 0.538. It is vital to maintain the I_2/H_2O ratio within this range so that the reactor effluence will consist of HIx solution with a composition well above the HIx azeotropic composition. If the effluence composition is too close to the azeotropic composition, then the separation of sulfuric acid and hydrogen iodide phases will not occur spontaneously in the L-L separator. Consequently, this in turn will cause problematic operations of Sections II and III.

The nominal operating pressures and temperatures corresponding to the minimum production rate specified above for the reactors involved are: (a) 100 kPa and 338 K for the Bunsen reactor, (b) 10,000 kPa and 1,123 K for the SA-IBSD reactor, and (c) 1,000 kPa and 760 K for the HI-DE reactor.

Lee et, al (2008) [11] proposed an optimum operating window for $I2/H2O$ molar feed flow ratio in Section I to be between 0.333 and 0.538. The objective to keep the I_2/H_2O molar feed ratio within the optimum range is to produce HIx (HI-I_2-H_2O mixture) effluence with a composition well above its azeotropic composition, which in turn will help achieve the following:

i. Enables spontaneous liquid-liquid (HI in I_2 and aqueous H_2SO_4) phase separation in the liquid-liquid (L-L) separator.
ii. Avoids the need for concentrating the HI gas (before decomposition reactor) using an energy-intensive unit, e.g., electro-electrodialysis (EED), or reactive distillation column.

Meanwhile, it is vital to retain the SA-IBSD reactor temperature below a maximum of about 1200°C but should remain above a minimum of 850°C to improve plant safety, reduce high-temperature energy utilization, and keep reactor conversion at an economical level. Note that, the SA-IBSD temperature must be kept high enough (above 850°C) to achieve a minimum reactor conversion of 36% [12]. A lower reactor conversion will lead to uneconomical operation of the reactor, hence the SITC process overall will become economically less favorable as it will consume an excessively large amount of high-temperature thermal energy (thermal efficiency will be too low). It should be pointed out that the temperature reaches the highest value at the reaction zone inside the SA-IBSD reactor. Therefore, one of the control objectives is to keep the reactor temperature at a setpoint between 850°C to 1200 °C.

In summary, there are several important constraints in the SITC plant operation: (a) minimum hydrogen production rate, (b) maximum temperature of the SA-IBSD reactor (in the reactive zone), and (c) minimum and maximum limits of I_2/H_2O molar feed ratio of iodine and water flowing into the Bunsen reactor. The specifications of these constraints are listed in Table 2. Furthermore, these constraints must not be violated to achieve smooth and safe operation.

Table 2. Major process constraints in the SITC plant.

Variables	Constraint Specification
Hydrogen flow rate, $\dot{m}_{H2}$ (kg/hr)	$\geq 1{,}000$
Temperature SA-IBSD reactor, $T_{SA-IBSD}$ (K)	$850\ to\ 1{,}200$
The ratio of feed molar flowrate I_2/H_2O, R_{nI_2/H_2O}	$0.33\ to\ 0.54$

3. PWC Methodology

The SOCS method is adopted to design the PWC strategy for the SITC plant. The SOCS procedure consists of two parts [13]–[15]:

i. Top-down analysis, including the specifications of operational objectives and degrees of freedom analysis. This analysis mostly focuses on the economics and steady-state evaluations of the given plant flowsheet.
ii. The bottom-up design of the control system starts with the design of the stabilizing (regulatory) control layer. This analysis focuses on the dynamic performance of the given plant.

Since the proposed industrial SITC plant flowsheet is new (is not yet exist in a real environment), the key variables that are strongly related to its performance are still unknown. To facilitate the search for these key variables, the Principal Component Analysis (PCA) based method by J. Nandong *et.al*, (2010) [16] is adopted to assist in the top-down analysis and bottom-up design. The PCA-based method is to identify the input-output variables that can give the desired self-optimizing control structure.

For this pseudo-industrial-scale plant, the PWC preliminary steps are applied to obtain initial information (e.g., total energy requirement) before applying the SOCS method. The proposed PWC preliminary steps (PWC Pre-Step) consist of the steady-state mass balance, analysis of total energy requirement, analysis of utilities, scaling-up of the SITC plant production rate, scaling-up of each unit and evaluating the process dynamics via dynamic simulation. These analyses are essential to ensure that the plant design and operation are reliable before proceeding to the detailed PWC design.

A reliable process model considering critical issues in process dynamics is needed to address the challenges in the SITC PWC design. Essentially, this model provides knowledge on process dynamics required in the design and control study of the plant. Therefore, the model-based analysis can systematically address the SITC problems. The kinetic data used for modelling the Bunsen reactor is from Q. Zhu *et al.* (2013) [17], and that for modelling the SA-IBSD reactor is from R. Moore *et al*. [12]. The details of all models for the three sections in the proposed plant flowsheet (Figure 2) are available in N. Mohd (2018) [18]. Figure 3 summarizes the modelling methodology for each unit in the SITC plant.

3.1. Process Scale-up

The scale-up of the SITC plant is to determine the appropriate dimensions of all the units involved to attain a minimum production rate of 1 ton/hr. Conducting the SITC plant scale-up is necessary for there is no existing industrial-scale SITC plant to be used for a direct reference (for unit dimensions). The scale-up of chemical processes is often a complicated task and could be very costly when it goes wrong due to unreliable data. Thus, process scale-up requires the art of designing a new plant using minimal data.

Several specific challenges related to the physical and chemical aspects of the process scale-up that have to be addressed are as follows:

1. **Reaction kinetics**: The SITC process involves several reaction kinetics parameters. These kinetics parameters are assumed to take similar values for the laboratory or experimental scale, and industrial-scale process. Thus, the parameter values from the laboratory scale are adopted in the industrial-scale plant.
2. **Chemical equilibrium**: A reversible reaction will not be practically productive until it attains chemical equilibrium. This attainment might not occur immediately or fast enough. Hence, the SITC reactions can reach equilibrium in shorter periods when higher

reactant concentrations are involved. However, the relationship between the equilibrium concentration and the equilibrium time is often highly nonlinear.

3. **Material properties**: The incorrectly selected materials can adversely influence the reactions, lead to the rapid degradation of equipment, or even make the system prohibitively expensive. The material of construction for the SITC plant is chosen based on reliable studies reported in the literature.
4. **Thermodynamics**: Heat loss or gain can play a significant role in chemical reactions. Controlling the reaction temperature is vital to ensure a successful plant scale-up. Thus, many of the control loops in the SITC plant focus on the temperature control objectives.
5. **Equipment selection and design**: The ratio of the surface area to mixture volume determines how quickly heat can discharge from the system, e.g., the reactor. If a reactor is not well designed, it can cause the control of chemical reactions involved difficult or impossible; the reactor condition might easily escalate or drift quickly from the desired value in the presence of an external disturbance, e.g., a drop in conversion. Furthermore, a correct design can avoid the snowball effect in the plant [19]. In the present study, the established procedures reported in the literature serve as guidelines for equipment selection and scale-up.

Based on the goal to achieve a minimum of 1,000 kg/hr of H_2 production, a backward calculation is performed as follows

$$\underbrace{13H_2O + 5I_2 + SO_2}_{Section\ I} \leftrightarrow \underbrace{H_2SO_4 + 5H_2O}_{Section\ II} \leftrightarrow \underbrace{4HI + 4I_2 + 6H_2O}_{Section\ III} \quad (4)$$

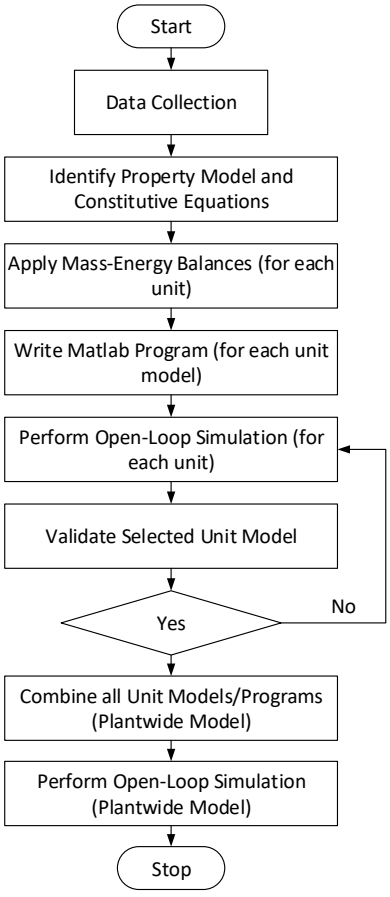

Figure 3. Flowchart of an overall modelling methodology for each unit in the SITC plant.

Figure 4 illustrates key steps in the SITC plant scale-up. By assuming 99% conversion in each Section II and Section III, the estimated total production rate of H_2SO_4 and HI mixture required to generate 1,000 kg/hr of hydrogen is 9,500 kg/hr. This hydrogen production rate is accomplished by setting the feed flow rates of water, iodine and sulfur dioxide accordingly into the Bunsen reactor. Once the desired feedstock amount is calculated, the size of the Bunsen reactor including its area and height can be optimized based on the estimated feed and production rate.

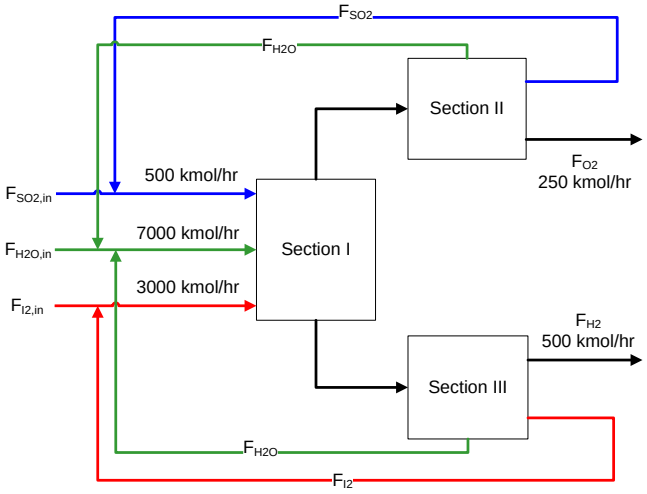

Figure 4. An illustrative block diagram of the SITC plant scale-up procedure.

3.2. Optimization

Response Surface Methodology (RSM) forms an essential part of the process optimization methodology. RSM is a method of sensitivity study that can help minimize the number of trials (simulation runs under different conditions) required to generate sufficient data to build a statistical model, which predicts interactions among the variables of interest with a given response variable, for example, the hydrogen yield. The RSM model serves as a simple tool to determine the potential candidate of manipulated variables (MVs) and controlled variables (CVs) needed to achieve the plant control objectives. In this study, the Design Expert (v9) software enables the statistical analysis of the RSM models. In addition to the analysis of RSM models, the PCA-based is also incorporated into the proposed methodology to analyze the critical input-output of the SITC plant, and to identify inputs and outputs that can lead to the self-optimizing property. The proposed sensitivity study and analysis via the RSM and PCA are summarized as follows:

1) **Step 1** – Generation of operating regimes. Select a nominal (0) operating level, and for each nominal level apply the step input changes to produce a set of data for the lower (-1) level and higher level (+1). The magnitude of input perturbation is selected based on the constraints (upper and lower limits) imposed on the input variable.
2) **Step 2** – Generate data. Compute the responses of the quality (response) variables corresponding to each operating level.
3) **Step 3a** – RSM Analysis. Gather and combine all the generated data on the process parameters, input-output variables and the computed response variables in Step 2. The Analysis of Variance, ANOVA and optimum operating condition are determined. Based on the ANOVA result, the significant input factors are selected as potential MVs while the significant response variables are selected as potential CVs.
4) **Step 3b**- PCA analysis. Gather and combine all the generated data on the process parameters, input-output variables and the computed response variables in Step 2. The plot of principal components (2D and 3D plots), as well as the Pareto plots, are generated. From these plots, the significant input factors can be identified and should be selected as the potential MVs while the significant response variables should be selected as the potential CVs.

Note that the sets of CVs and MVs obtained in Step 3a may not be the same as those obtained in Step 3b. The main idea is to identify a suitable set of manipulated variables for controlling the selected output variables so that the control structure will exhibit the best self-optimizing property.

3.3. Cost Analysis

The minimization of equipment costs and other expenses related to capital investment is essential in plant design. The capital costs of a new-fangled plant comprise primarily of Fixed Capital Investment (FCI), land cost, and working capital costs. Keep in mind that the FCI consists of the equipment purchase

cost, which refers to as the Bare Module Cost (BMC) and includes all the necessary additional expenses to construct the plant. These additional costs associated with the BMC are the sum of the direct and indirect costs of the purchase price. Direct costing covers the material, labour, and equipment costs. Meanwhile, indirect costing includes freight, insurance, taxes, construction, overhead, and contractor engineering expenses.

The BMC is defined as follows:

$$C_{BM} = C_P F_{BM} \tag{5}$$

where C_{BM} is the bare module equipment cost including the direct and indirect cost for each unit, C_P is the purchase cost for the base condition including equipment made of the most common material, usually carbon steel and operating at near ambient pressure, and F_{BM} is the bare module cost factor.

3.4. Plantwide Control Design Procedure

The summary of the PWC design is shown in Figure 5. The PWC structure will be selected using a systematic procedure described below:

1. Identification of control objectives and constraints.
2. Input-output identification. The Input-output identification is generally included as part of the modelling and simulation procedure. Process model optimization and sensitivity study method are used to identify the potential inputs as the manipulated variables (MVs) and the outputs as controlled variables (CVs).
3. Selection of control structure whether decentralized or centralized or mixed of both.
    a. Decomposition into major plant sections.
    b. Selection of control laws and synthesis methods, e.g., controller synthesis using IMC-PID, MSC-PID, NMPC, etc.
    c. Evaluation of each section or unit via a simulation study.
4. Assembling of PWC structure. All of the control strategies of each section (i.e., in step 3) are assembled to develop the complete PWC structure. The Self-Optimizing Control Structure (SOCS) is chosen as the PWC structure for the plant.
5. Plantwide optimization. The developed PWC structure is optimized considering both steady-states and dynamics performance criteria. This is to achieve a good between these two conflicting criteria.
6. Pre-evaluation of the PWC structure.
7. Enhancement of the PWC structure.
8. Evaluation of the refined PWC control strategy.
9. Stop after meeting all of the specified control objectives and constraints.

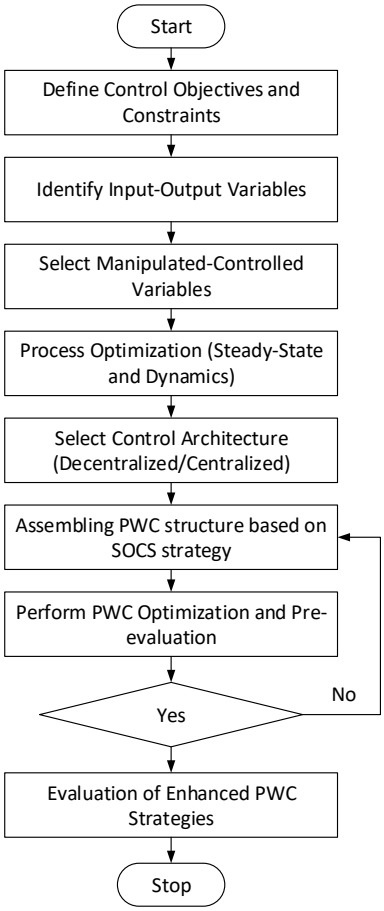

Figure 5. Flowchart of the overall PWC structure development.

3.5. Optimal-Practical Plantwide (OPPWIDE) Optimization

The OPPWIDE optimization aims to achieve a trade-off between optimality and practicality. For this reason, the cost function ($J_{oppwide}$) for the optimization is a weighted function in terms of the steady-state economic criterion (optimality) and dynamics controllability criterion (practicality) of the SITC plant. Figure 6 presents the flowchart of the proposed OPPWIDE optimization methodology. The optimality feature identifies the optimum values of the operating and design parameters that meet desired economic performance. The objective is to assess the effect of controlling each variable on the plant operation to achieve optimum plant profit. Meanwhile, the practicality feature is based on a new Loop Gain Controllability (LGC) index [18]. Note that, a higher LGC value suggests that the given plant is easier to control, i.e., a simpler and cheaper control system can be used.

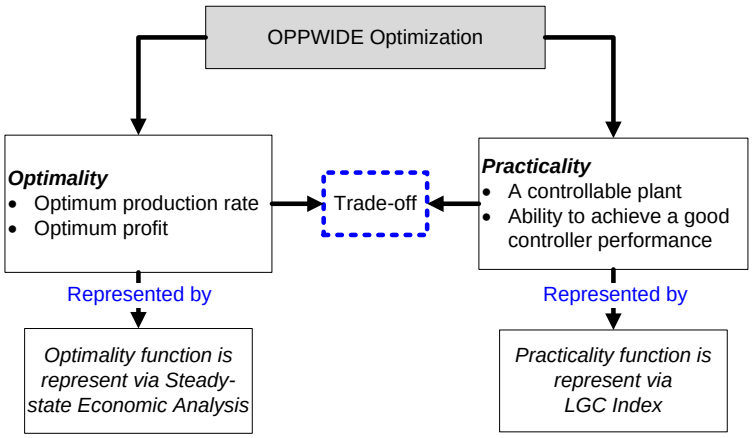

Figure 6. Brief description diagram of OPPWIDE optimization methodology.

The Twin Plot self-optimizing control structure (SOCS) method is one of the tools used in the OPPWIDE optimization procedure. The objective of the Twin Plot SOCS method is to obtain a self-optimizing cost function (*J*) of the given plant. There are two plots involved in this method: (1) Skogestad SOCS plot, and (2) PCA loading plot.

Figure 7 shows a Skogestad SOCS plot. This plot illustrates the loss (e.g., profit) imposed by changing the setpoint of a CV. It is desired that the cost function is kept at an optimal value despite the occurrence of a disturbance or change in the setpoint. This idea is known as 'self-optimizing control. In Figure 7, the one with a smaller amount of loss (less sensitive to the change in CV) is a superior choice of the cost function. In this case, J_B has a smaller amount of loss as compared to J_A over the same range of CV change. The next step is to find the manipulated variable (MV) to obtain a self-optimizing cost function of J_B. The selection of MV is based on the second plot - the PCA loading plot.

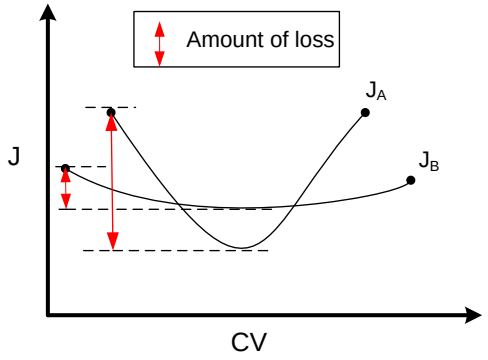

Figure 7. Skogestad SOCS plot: economic loss function (J) against the controlled variable

Figure 8 illustrates the PCA plot of principal components 1 and 2. The PCA plot consists of four quadrants, i.e., quadrants A, B, C, and D. The variables in quadrant A are deemed to have opposite trends (negatively correlated) to that in D but the variables within the same quadrant are positively correlated among themselves. Similarly, the variables in quadrant B will have opposite trends to that in C (negatively correlated). The variables located within quadrants A and D are not correlated (very weak interactions) with the variables within quadrants B and C. There are two criteria for the correlation of a significant variable: (a) variables in the same quadrant and (b) variables in the opposite quadrant. As can be seen from Figure 8, quadrant B has three variables, two are candidates for the controlled variable 1 (CV1), controlled variable 2 (CV2), and another is the cost function *J*. Based on this plot, one may deduce that *J*, CV1, and CV2 (in quadrant B) are negatively correlated with the potential manipulated variables MV1 and MV2 (in quadrant C). Since they are in the opposite quadrants, an increase in MV1 or/and MV2 will lead to a decrease in *J*, CV1, and CV2, or vice versa. The distance (length) of each variable from the origin represents a coefficient value. A greater length of a variable from the origin represents a higher coefficient value, thus a stronger influence. Hence, it has a more significant influence on the variables in the opposite quadrant and those in its quadrant. In this case, CV1 has a more significant effect on the cost function *J* as compared to CV2. Therefore, CV1 should be chosen as the primary control variable. To control CV1, a selection of manipulated variables should be obtained from quadrant C. Here, the MV2 has a smaller PCA coefficient than MV1 (see Figure 8; MV2 is shorter than MV1) indicating that MV2 has a smaller correlation with *J* as compared to MV1. Hence, MV2 is a preferable manipulated variable for CV1 as its adjustment will lead to a smaller loss in *J* (than if MV1 is adjusted). As a result, a self-optimizing cost function can be obtained by choosing J_B as a function of CV1 and MV2.

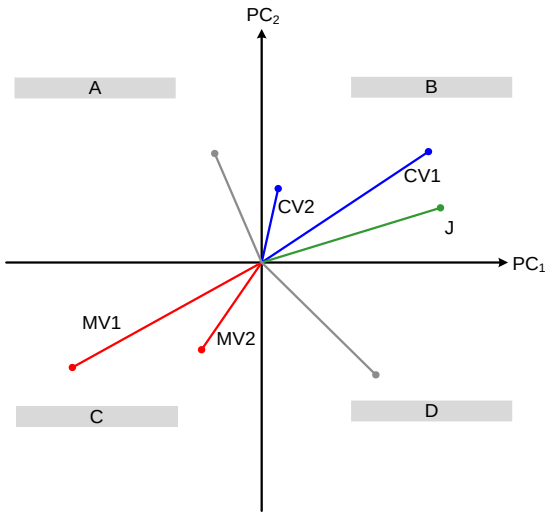

Figure 8. PCA plot of the first and second principal components.

The manipulated variables and controlled variables for evaluating the LGC index are selected based on the Twin Plot SOCS method. This method helps reduce the number of variables in the PWC structure. Hence, it can save computational time (due to reduced complexity) and simulation effort. The integration of the Twin Plot SOCS method and LGC index in the OPPWIDE optimization method is unique. This new approach can provide an efficient way to perform the given PWC optimization by reducing PWC complexity.

4. Results and Discussion

4.1. PWC preliminary steps (pre-steps)

The results of the PWC pre-step analysis are detailed as follows.

PWC Pre-Step 1: Identifying steady-state mass balance

The steady-state mass balance analysis is vital to identify the total inflows and outflows of the entire plant regardless of whether it is dynamic. The steady-state mass balance equation is expressed by:

$$F_{H2O_i} + F_{I2_i} + F_{SO2_i} = F_{H2_e} + F_{O2_e} + F_{H2O_e} + F_{I2_e} + F_{SO2_e} \quad (6)$$

where F_{H2O_i}, F_{I2_i}, F_{SO2_i}, F_{H2_e}, and F_{O2_e} denote the overall flow rates (unit: kg/hr) of water, iodine, sulfur dioxide, hydrogen and oxygen respectively. The subscript 'i' and 'e' indicate inflow and outflow from the plant.

PWC Pre-Step 2: Analysis of total energy

In this step, the objective is to estimate the total energy requirement by the SITC plant, H_{TE} necessary to meet the desired conversion. Table 3 shows the operating conditions and amount of energy required in the Bunsen reactor. The energy to be absorbed by the cooling jacket of the Bunsen reactor is calculated as follows.

Section I (Exothermic):

$$H_{E1} = F_{cE1} C_{pE1} (T_{BRexit} - T_{cE1}) \quad (7)$$

where the notations are shown in the nomenclature.

Table 3. Bunsen reactor parameters and values.

Bunsen Reactor	Value
Energy absorbed by the jacket, Q_{BR} or H_{E1}	2.419 kJ/hr
Operating temperature, T_{BR}	60°C to 120°C
Exit temperature, $T_{BR_{exit}}$	60°C to 120°C

Based on the calculation in (7), the energy to be absorbed by the jacket at the reactor temperature between 60°C to 120°C is 2.419 kJ/hr. Table 4 lists the energy requirement and operating conditions of the SA-IBSD reactor. The energy required in the SA-IBSD reactor is calculated below.

Section II (Endothermic):

$H_{E2} = Thermal\ energy$ (7)

In (8), the general term thermal energy is used since the heating source is not finalized, i.e., it could be either from a nuclear power station or solar energy.

Table 4: SA-IBSD reactor parameters and values.

SA-IBSD Reactor	**Value**
The energy required, $Q_{SA-IBSD}$ or H_{E2}	5.1×10^8 kJ/hr
Operating temperature, $T_{SA-IBSD}$	800°C to 950°C
Exit temperature, $T_{SA-IBSD_{exit}}$	800°C to 950°C
The energy released at exit temperature, $Q_{HE2_{SA-IBSD}} = F_{pE2}C_{pE2}(T_{SA-IBSD_{exit}} - T_{SA-IBSD})$	2.9×10^9 kJ/hr

For the SA-IBSD reactor, the specified amount of supplied energy means the amount needed to achieve the desired reactor conversion. The energy required by the SA-IBSD reactor from an external thermal energy source is $5.1\times 10^8\ kJ/hr$. Table 5 lists the operating conditions and energy required for the Hydrogen Iodide, *HI* Decomposer. The calculation of energy required is essential to ensure that the energy integration between *HI* decomposer and SA-IBSD reactor is feasible. The heat integration is feasible only if there is more energy remaining after the *HI* decomposer utilizes it. The required energy by the *HI* decomposer is calculated as follows.

Section III (Endothermic):

$H_{E3} = F_{sE3}C_{psE3}(T_{sE2} - T_{HI-DEexit})$ (8)

Table 3. HI Decomposer parameters and values.

HI Decomposer	**Value**
Energy required, Q_{HI-DE} or H_{E3}	9.5×10^4 kJ/ht
Operating temperature, T_{HI-DE}	450 °C to 500 °C
Exit temperature, $T_{HI\_DE_{exit}}$	450 °C to 500 °C
Balance energy remains, $Q_{HI-DE_{add}} = Q_{HI-DE} - Q_{HE2_{SA-IBSD}}$	2.9×10^9 kJ/hr

From the calculation in (9), it is known that the energy required to decompose hydrogen iodide is $9.5 \times 10^4\ kJ/hr$. This amount of energy required is less than the energy able to be supplied by the exiting thermal medium from the SA-IBSD reactor in Section II. The total energy, H_{TE} required by the SITC plant overall is given by

$$H_{TE} = H_{E1} + H_{E2} + H_{E3} = 5.011\times 10^8 kJ/hr \quad (9)$$

Based on the energy analysis, it is shown that the heat integration between Sections II and III is feasible. The total energy released by Section II is $2.9 \times 10^9\ kJ/hr$. This amount is sufficient for the energy required in Section III, which is only $9.5 \times 10^4\ kJ/hr$. For Section I, there is no additional energy required since it is an exothermic reaction.

PWC Pre-Step 3: Analysis of utilities

Based on the calculated energy requirement, H_{TE} in the previous step, the required utility energy, E_T can be estimated as follows:

$$H_{TE} \cong E_T = 139kWh \quad (10)$$

PWC Pre-Step 4: Scale-up of SITC plant production

Before applying the detailed scale-up procedure, first design each piece of equipment individually based on the laboratory scale (i.e., experimental data available for validation). After completing the design of all laboratory-scale units, integration of the units according to the design flowsheet follows. Thus, the laboratory scale of the plant is developed and then simulated for validation with the available experimental data and to explore the plant dynamics. In this work, the target production rate is a minimum of 1 ton/hr of hydrogen.

PWC Pre-Step 5: Scale-up equipment unit

After deciding the desired minimum production rate, the unit scale-up follows accordingly. The scale-up for the units is listed in Table 6.

Table 4. The scale-up dimensions of the SITC units.

Equipment	**Maximum volume**
Bunsen Reactor (R-001)	300 m^3
Liquid-Liquid Separator (V-001)	500 m^3
Sulfuric Acid Flash Tank (V-002)	1,500 m^3
SA-IBSD Reactor (R-002)	400 m^3
Hydrogen Iodide Flash Tank (V-003)	1,500 m^3
HI Decomposer (R-003)	200 m^3

PWC Pre-Step 6: Dynamic modelling and MATLAB program simulation

Note that the dynamic modelling of each unit follows the fundamental modelling approach. Next is to write down MATLAB codes of the constructed dynamics models on m-files, which enable the use of s-functions in the MATLAB Simulink environment to represent the SITC plant simulation via the MATLAB Simulink.

4.2. Detailed PWC Development and Analysis

4.2.1. Cost Function and Constraints

One of the primary objectives of the PWC strategy is to achieve the desired performance as pre-defined by the scalar cost function J, which should be minimized. A typical cost function is represented by J = cost feed +cost utilities + product value. The cost function J can be written in the following form:

$$PR = -J = p_p P - p_{F_o} F_o - p_V V - p_D D \quad (11)$$

where the notations are explained in the nomenclature.

The fixed and capital costs are not in the objective function since they have a short (hourly) timescale. Hence, they are considered steady-state and do not affect the optimization [13]. Table 7 shows the prices ($/kg) involved. The utilities considered are electricity, process and cooling water, and the by-product credit (in this case oxygen).

Table 7. The products, feedstock and utility prices.

Item	**Price (≈$/kg)**
Products	
Hydrogen, H_2	3.76 [20]
Oxygen, O_2	1.50
Total	5.26
Feedstock [21]	
Water, H_2O	-
Sulfur dioxide, SO_2	-
Iodine, I_2	-
Total	0.38
Utilities [21], [22]	
Total	0.11

Based on the calculation in equation (11) and information in Table 7, with the assumption that at least 99% of feedstock (water, sulfur dioxide, and iodine) are recycled under the minimum hydrogen production rate, the steady-state cost function J, or equal to gross profit PR is,

$$PR = -J = (5.26)(1140) - (0.38)(3900) - (0.11)(139) = 4499 \ \ US\$ / hr$$

The minimum gross profit PR estimated based on equation (11) is US$ 35,632,080 per annum. This value considers an estimated price of thermal energy supplied via solar energy for Section II [22].

4.2.2. Control Degree of Freedom (CDOF) Analysis

The next step in the PWC structure design is to determine the number of control degrees of freedom (CDOF), which is a step ahead after carrying out the degree of freedom (DOF) analysis. The purpose of determining the CDOF is to find out the number of input variables that can be manipulated. In many cases, the CDOF (N_m) is equal to the number of manipulated variables [23]. One of the techniques for analyzing the CDOF is using the flowsheet-oriented method by N. V. S. . Murthy Konda and G. P. Rangaiah (2012) [24]. This technique is briefly explained by,

$$N_m = N_{streams} - \sum_1^{n_u} N_{restraining} - N_{redundant} \quad (12)$$

where n_u denotes the total number of units in the process plant. The meanings of $N_{redundant}$ and $N_{restraining}$ are as explained in [23]. Once the N_m is obtained, another analysis is carried out, which is the optimization of the degrees of freedom (ODOF), i.e., N_{ss}. The ODOF is the degrees of freedom that have an impact on the specified cost function, J ($US\$/hr$) and is given by,

$$N_{SS} = N_m - \left(N_{om} - N_{oy}\right) \quad (13)$$

Here, N_{0m} is the number of manipulated (input) variables, which ideally shall have no steady-state effect on the cost function. On the contrary, N_{0y} is the number of output variables that need to be controlled and ideally shall have no steady-state effect on the plant cost. Table 8 displays the CDOF of the SITC plant. There are at most 19 CDOF and 14 ODOF identified for the SITC plant. Following the identification of 14 ODOF, the next task is to identify the output variables based on the N_{ss} values. The controlled variables are shown in Table 9. The complete control structure of the industrial-scale SITC plant is shown in Figure 9.

Table 5. Calculated CDOF of the SITC plant.

DOF of SITC Plant	N_m	N_{0m}	N_{0y}	N_{ss}
Section I	7	0	3	4
Section II	7	0	1	6
Section III	5	0	1	4
Total	**19**	**0**	**5**	**14**

Table 9. Controlled variables, manipulated variables and controllers [25]

No	Controlled Variable	Manipulated Variable	Controller Type
Section I			
1	Bunsen reactor (R-001) temperature	Feed flow rate of cooling water	NMPC
2	Bunsen reactor (R-001) conversion	Feed flow rate SO_2	NMPC
3	Bunsen reactor (R-001) level	Total feed flow rate	PID
4	Heavy phase level in L-L separator (V-001)	Outlet heavy phase flow of L-L separator	MSC
5	Light phase level in separating chamber of L-L separator (V-001)	Total recycle flowrate	MSC
Section II			
6	H_2SO_4 flash tank (V-002) temperature	Feed flow rate of heating element 1	PID
7	H_2SO_4 flash tank (V-002) level	Feed flow rate to flash tank	PID
8	SA-IBSD reactor (R-002) temperature	Feed flow rate of the external jacket	MSC
Section III			
9	HI flash tank (V-003) temperature	Feed flow rate of heating element 2	PID
10	HI flash tank (V-003) level	Feed flow rate to flash tank	PID
11	HI decomposer (R-003) temperature	Feed flow rate of the heating element	NMPC
12	Hydrogen production rate	Feed flow rate I_2/H_2O	NMPC

NMPC = nonlinear model predictive controller
MSC = multi-scale controller
PID = proportional-integral-derivative controller

4.2.3. Primary Controlled Variables Identification

The yields of the main product (hydrogen) and by-product (oxygen) are affected by the Bunsen reactor (BR) holdup liquid level, BR temperature, L-L separator holdup liquid levels, sulfuric acid flash tank (SA-FT) holdup liquid level, SA-FT temperature, external jacket temperature of SA-IBSD reactor, the temperature of SA-IBSD and temperature of HI-DE reactor. Note that because all these output variables significantly affect the process operation, controlling them at desired values is vital to ensure profitable and smooth operation.

4.2.4. Selection of Throughput Manipulator Location

Finding the appropriate throughput manipulator (TPM) location is crucial as it links the top-down and bottom-up parts of the SOCS procedure [13]. The TPM location is selected based on the PCA result. The PCA result reveals that the feed I_2/H_2O molar ratio is the most significant input affecting the SITC plant production. Therefore, the first TPM is chosen as the feed I_2/H_2O molar ratio. Table 10 shortlists the potential inputs for the TPM based on the PCA result. By optimization one can deduce that the significant input variables shall have significant effects on the oxygen and hydrogen production rates.

From the analysis of significant variables, both T_{oBR} and F_{SO2oBR} of the Bunsen reactor are identified as the potential inputs for the TPM. Since FJ_{SAIBSD} is a utility flow rate, it is not suitable as the manipulated input for the TPM controlling the hydrogen production rate. As mentioned in [13], the objective of TPM is to determine the amount of mass flow through the plant which can usually be expressed as a feed rate or production rate. Hence by referring to the PCA result, the significant mass flow affecting the hydrogen production is found to be the iodine and water feed flows to the Bunsen reactor.

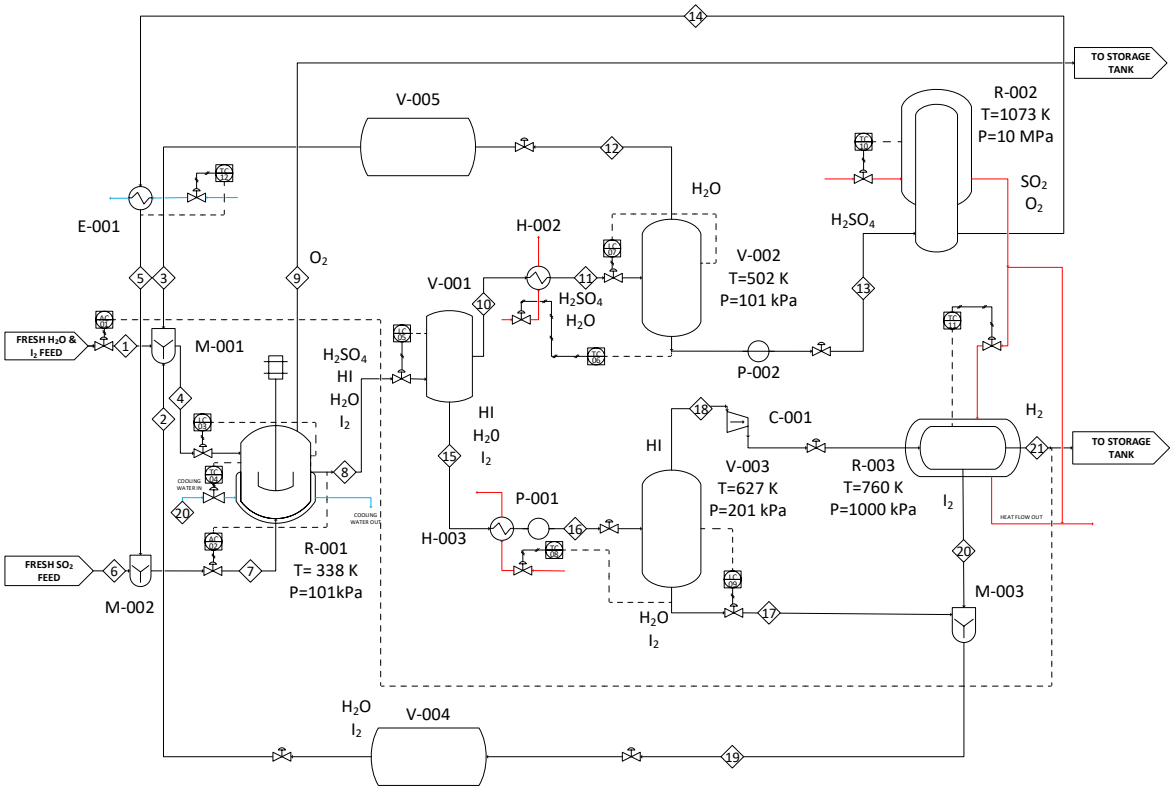

Figure 9. The proposed control loops for the pseudo-industrial-scale SITC plant.

Table 10. The prospective inputs for the TPM based on the PCA result.

Output	Potential Input	PCA Coefficient
Oxygen Flowrate	A: T_{oBR}	0.0013
	E: F_{SO2oBR}	0.00076
	J: FJ_{SAIBSD}	-0.00038
Hydrogen Flowrate	A: T_{oBR}	-0.03
	E: F_{SO2oBR}	-0.00275
	J: FJ_{SAIBSD}	-0.0189

As the reactor operating condition (i.e., temperature) should be fixed through optimization, the sulfur dioxide feed flow rate is found to be the best choice as the second input for the TPM of the SITC plant. Please note that it is quite common to have more than one TPMs for a given plant. Since both the feed I_2/H_2O molar ratio ($N_{I2/H2O}$) and feed sulfur dioxide flowrate F_{SO2oBR} are introduced into the Bunsen reactor, it is possible to reduce these two TPMs into a single TPM by specifying an optimal feed ratio of both TPMs, i.e., the ratio of feed I_2/H_2O to sulfur dioxide flowrate or choosing only one TPM (either feed I_2/H_2O or sulfur dioxide flow rate). Here, the latter approached is adopted for the SITC plant.

4.2.5. Selection of Regulatory Control Structure

The regulatory control layer aims to stabilize the given plant. For the SITC plant, analysis of the plant dynamics suggests that the regulatory control goal is achievable through controlling the Bunsen reactor liquid level, L-L separator liquid level, and flash tank liquid levels. Note that the supervisory control layer will provide remote setpoints to the regulatory control layer. Keep in mind that the supervisory control layer might involve the direct imposition of several constraints through override control strategy or via advanced model-based control strategy such as Model Predictive Control (MPC).

4.2.6. Selection of Supervisory Control Structure

The objective of the supervisory control layer is to control the primary production in the SITC plant – to achieve desired overall control performance. Note that the supervisory control layer and economic

performance of the given plant are often linked. By properly selecting the supervisory controlled variables, one can ensure a strong link between the supervisory control layer and economic performance. For this reason, the oxygen and hydrogen production rates and the reactor temperatures should be the controlled variables for the supervisory control layer. Due to tight input-output constraints attached to this layer, an advanced nonlinear NARX-MPC (NMPC) controller is preferable to the standard multi-loop PID control for controlling the oxygen and hydrogen flow rates.

4.2.7. Selection of Optimization Layer

Table 11 shows the optimization results of two SITC models. The SITC plant of Model 1 is optimized based on the proposed PWC structure. The SITC plant of Model 2 is optimized solely based on sensitivity study analysis. Based on Model 1, the calculated LGC index is 0.1096. This value indicates that Model 1 is controllable since it is a positive value. Note that the smaller the value of LGC (less than unity), the harder it will be to control the given system using a conventional PID controller. Notice that the LGC value based on Model 1 is small, implying that the system is controllable, but the maximum achievable control performance is low. The calculated profit corresponding to Model 1 is US$ 8,070 per hour, hence showing that Model 1 is a profitable model scheme. The profit (economic) of Model 2 is comparable to that of Model 1. However, for Model 2, the LGC is negative. This negative LGC value implies that the system based on Model 2 is not controllable. Therefore, a profitable plant may not necessarily lead to a controllable plant. By applying the proposed optimization method, it is possible to detect and select a favourable operating regime or plant scheme (model) which leads to a profitable and controllable system – hence guaranteeing a viable plant operation and design. Moreover, this control structure strategy can meet the optimality (economic) and practicality (controllability) performance criteria.

Table 11. Performance assessment of the SITC plant based on the OPPWIDE analysis.

SITC model		**Controllability performance (LGC) (ψ_1)**	**Economic performance ($/hr H_2) (ψ_2)**
Model 1			
MV1: Feed molar ratio I_2/H_2O MV2: Feed flowrate sulfur dioxide	CV1: Hydrogen flowrate CV2: Temperature HI-DE (R-003) reactor	0.1096	8,070
Model 2			
MV1: Feed molar ratio I_2/H_2O MV2: Feed flowrate sulfur dioxide	CV1: Hydrogen flowrate CV2: Temperature HI-DE (R-003) reactor	-1.009	8,019

4.3. PWC robustness Evaluation

To evaluate the closed-loop robustness of the nonlinear MPC (NMPC) scheme used in the supervisory control layer, a load change (30%) is introduced at t = 300hr lasting for 100 hours, to the TPM at the Bunsen reactor. Figure 11 shows that the controller takes a while to reject the disturbance but remains able to drive the hydrogen flow rate to its desired set point. Even under the introduction of the load change, the controller can still maintain the hydrogen flow rate, i.e., meeting the PWC objective where it is desirable to maintain the hydrogen production rate at or more than 1,000 kg/hr. Figure 12 shows the MV profile corresponding to the robustness test. Keep in mind that the controller does not violate the input constraints. These results prove that the NMPC controller is robust in the face of load change to the TPM. The robustness of the NMPC controller verifies that the selection of TPM is appropriate for the self-optimizing control structure.

Another test is for the setpoint tracking performance. The objective of the setpoint tracking test is also to evaluate the robustness and performance of the NMPC which controls both hydrogen iodide mixture, $HIx/(HI + H_2O)$ and hydrogen flow rate, m_{H2} (in Section III). Figures 13 and 14 demonstrate that the NMPC can drive the ratio of hydrogen iodide mixture, $HIx/(HI + H_2O)$ and hydrogen flow rate, m_{H2} to their desired setpoints respectively, with a fast response and short time delay.

The spikes in the controlled variable (CV) profiles are due to the implementation of a constraint on the NMPC on the manipulated variable (MV). Liuping (2009) reports that the spike shown in the MV profile is quite a common phenomenon in MPC. Figure 15 shows the MV profile and its upper and lower limits. Interestingly, the MV (feed molar ratio) does not violate the specified limits where the lower limit is 0.32 while the upper limit is 0.54.

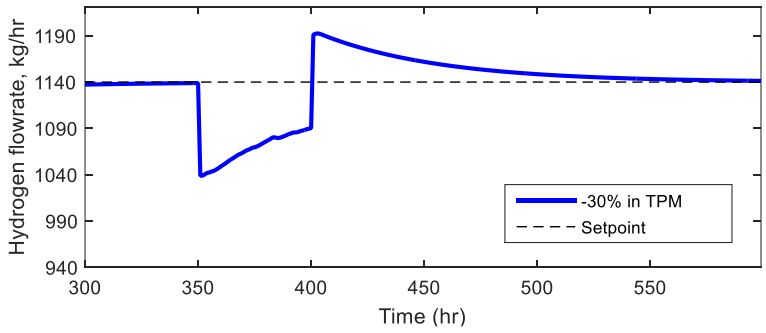

Figure 11. Hydrogen flowrate profile of NMPC for -30% load change in the TPM on hydrogen flow rate.

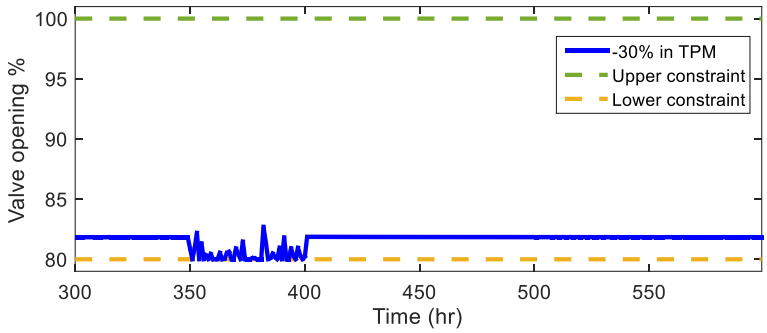

Figure 12. MV profile of NMPC for -30% load change in the TPM.

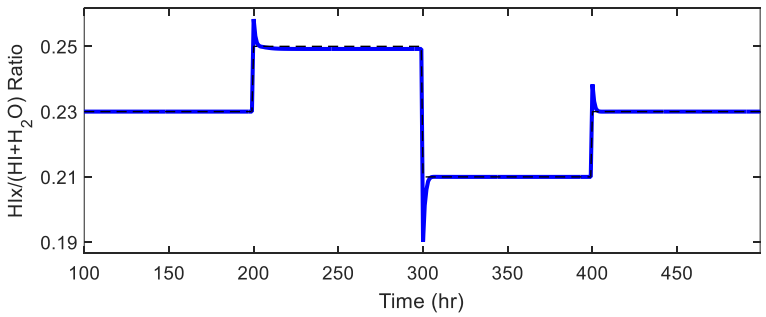

Figure 13. *HIx* mixture (CV1) profile of NMPC for setpoint change on the ratio of hydrogen iodide mixture.

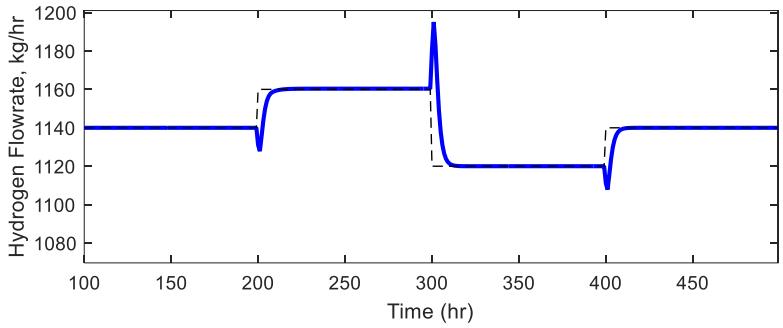

Figure 14. Hydrogen flowrate (CV2) profile of NMPC for setpoint change on hydrogen flowrate.

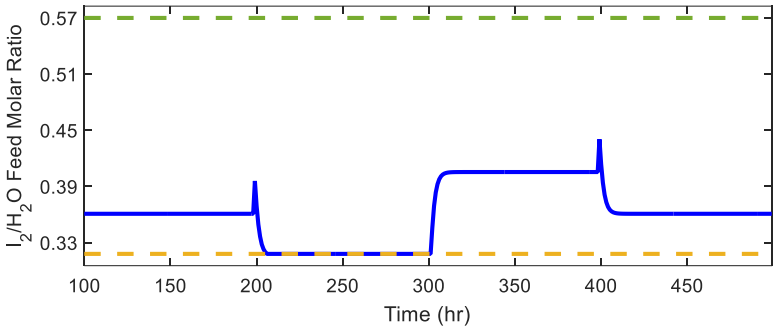

Figure 15. MV profile of NMPC for setpoint change on the feed I_2/H_20 molar ratio.

4.4. SITC plant performance assessment

In 2012, R. Liberatore *et al.* (2012) [22] carried out economic and energy analyses for a solar energy-based industrial-scale SITC plant. The SITC plant by R. Liberatore *et al.* (2012) [22] has a production capacity of 100 metric tons/day of hydrogen where the production cost is 10.25 $/kg-H2. By applying the SOCS-based PWC structure to the presently developed industrial-scale SITC plant, the thermal efficiency η that can achieve a maximum production rate of hydrogen of 2,400 kg/hr H2 (or 57.6 tonnes/day):

$$\eta = \frac{H_{HHV}}{H_{heat\ 2400\,kg/hrH2}} = \frac{285.8\ kJ/mol}{416.7\ kJ/mol} H_2 = 0.686 \tag{14}$$

Meanwhile, at the production rate of 1,140 kg/hr (or 27.4 tonnes/day):

$$\eta = \frac{H_{HHV}}{H_{heat\ 1140\,kg/hrH2}} = \frac{285.8\ kJ/mol}{869.6\ kJ/mol} H_2 = 0.329 \tag{15}$$

Note that, H_{HHV} denotes the higher heating value of H_2 fuel and H_{heat} denotes the heat required to produce the desired hydrogen production rate (calculated based on the preliminary PWC steps).

As shown by the above calculations, the achievable thermal efficiency for the proposed SITC plant lies between 32.9% and 68.6%. By applying process optimization and efficient controller design, the plant's thermal efficiency can increase beyond the currently reported maximum value in the literature. The gross profit is estimated to be US$ 35,632,080 per annum with a hydrogen production cost of 4.19 $/kg (based on 24 tonnes/day). The production cost estimation assumes that the external heating energy for Section II is similar to the value in [22] where the hydrogen production cost was 9.37 $/kg (100 tonnes/day). Meanwhile, [2] estimated the hydrogen production cost at 4.47 $/kg (based on 100 tonnes/day). Compared to the works of R. Liberatore *et al.* (2012) [22] and C. Huang and A. T-Raiss (2004) [2], the application of the SOCS-based PWC strategy can substantially help reduce the production cost of hydrogen via the SITC process. Besides, if the proposed strategy is applied to a SITC

plant where the SA-IBSD is integrated to fuel cell stacks, it is estimated to have lower production cost and more profit where a high yield of around 57% at a lower operating pressure and gas temperature of 1025 K as has been reported by S. Skogestad (2000) [26]. This reduction is possible due to the self-optimizing property of the plant control structure, where the configurations of the supervisory and regulatory layers tend to minimize the loss of the cost function associated with the reactor operations (manipulated variables) [27].

5. Conclusion

This paper addressed the gap in the limited study reported for the design and PWC simulation of an industrial-scale of the Sulfur-Iodine Thermochemical Cycle (SITC) plant. The contributions to the research area involved are the proposed PWC preliminary steps and OPPWIDE optimization methodology. These contributions are essential for developing the plantwide self-optimizing control structure (SOCS) for the pre-defined SITC flowsheet. By adopting the plantwide SOCS strategy, the scaled-up SITC plant can provide thermal efficiency ranging from 32.9% to 68.6%, determined at the production rate of 27.4 tonnes/day and maximum production rate of 57.6 tonnes/day, respectively. Presently, the highest thermal efficiency for a SITC plant reported in the literature is 34%. Extensive simulation of the SITC plant has shown that the optimized plantwide SOCS strategy can provide better performances than the unit-based PWC strategy in terms of controllability and economic criteria. A nonlinear MPC (NMPC) has been chosen for the supervisory level to control the TPM located at the Bunsen reactor (R-001) (Section I). The reason for adopting NMPC is due to the tight input-output constraints associated with the operation of the Bunsen reactor. The robustness test via simulation proved that the SITC plant under the given SOCS strategy is flexible enough to cope with a significant change in disturbance and setpoint changes. At the minimum production rate of about 24 tonnes/day of hydrogen, the SITC plant can attain a gross profit of US$ 35.6 million per annum leading to a hydrogen production cost of 4.19 $/kg-H2. In conclusion, the pre-defined SITC flowsheet is viable on the grounds of both economic and controllability. Note that the PWC development for the SITC plant posed a significant limitation, due to unknown parameters and the lack of fundamental understanding of the process at an industrial scale. In future, the research shall be expanded into developing a complete scale-up design specification for all major and minor equipment according to the engineering standard, proposing advanced process integration, and exploring a more economical and sustainable energy source for the industrial-scale SITC plant.

Nomenclature

C_{pE1}	Bunsen reactor: Specific heat capacity
C_{pE2}	SA-IBSD reactor: Specific heat capacity
C_{psE3}	HI-DE reactor: Heat capacity
F_{cE1}	Bunsen reactor: Cooling water flow rate
F_{pE2}	SA-IBSD reactor: Heating medium flow rate
F_{sE3}	Heating element flow rate (from the SA-IBSD reactor to HI-DE reactor)
N_{0m}	Number of manipulated (input) variables
N_{0y}	Number of output variables
T_{cE1}	Bunsen reactor: Cooling water temperature
T_{sE2}	SA-IBSD reactor: Outlet temperature of heating element
T_{c2}	Bunsen reactor: Outlet temperature
$p_D(US\$/kg)$	Recycle cost
$p_{Fo}(US\$/kg)$	Feedstock price
$p_V(US\$/kg)$	Energy cost
$p_p(US\$/kg)$	Product price
λ_{E3}	HI-DE reactor: Sensible heat.
BR	Bunsen Reactor
CDOF	Control Degree of Freedom
CV	Controlled Variable
DOF	Degree of Freedom

H_{heat}	The heat required to produce the desired hydrogen production rate
H_{HHV}	Highest heating value
HI-DE	Hydrogen Iodide Decomposer
LGC	Loop Gain Controllability
LLS	Liquid-liquid Separator
MSC	Multi-Scale Controller
MV	Manipulated Variable
NMPC	Nonlinear Model Predictive Controller
ODOF	Optimization Degree of Freedom
OPPWIDE	Optimal-Practical Plant-Wide
PCA	Principal Component Analysis
PID	Proportional Integral Derivative controller
PWC	Plantwide Control
SA-FT	Sulfuric Acid Flash Tank
SA-IBSD	Sulfuric Acid Integrated Boiler Superheater Decomposer
SITC	Sulfur-Iodine Thermochemical Cycle
SOCS	Self-Optimizing Control Structure
TPM	Throughput Manipulator
$PR(US\$/kg)$	Profit

Acknowledgement

The financial support from an FRGS grant (no: JPT.S Jld.13(28)) of the Ministry of Higher Education (MOHE), a CMRI grant from Curtin University Malaysia, a scholarship from the Ministry of Education (MOE) and an XMUMRF grant (no: XMUMRF/2021-C7/IENG/0035) of Xiamen University Malaysia are greatly acknowledged.

References

[1] C. Huang and A. T-Raissi, "Analysis of sulfur-iodine thermochemical cycle for solar hydrogen production. Part I: Decomposition of sulfuric acid," *Sol. Energy*, vol. 78, no. 5, pp. 632–646, 2005, doi: 10.1016/j.solener.2004.01.007.

[2] R. Perret, "Solar Thermochemical Hydrogen Production Research (STCH) Thermochemical Cycle Selection and Investment Priority," *Sandia Rep.*, no. May, pp. 1–117, 2011.

[3] N. Hiroki *et al.*, "Hydrogen production using thermochemical water-splitting Iodine–Sulfur process test facility made of industrial structural materials: Engineering solutions to prevent iodine precipitation," *Int. J. Hydrogen Energy*, vol. 46, no. 43, pp. 22328–22343, 2021.

[4] S. Kasahara *et al.*, "Current R&D status of thermochemical water splitting iodine-sulfur process in Japan Atomic Energy Agency," *Int. J. Hydrogen Energy*, vol. 42, no. 19, pp. 13477–13485, 2017, doi: 10.1016/j.ijhydene.2017.02.163.

[5] K. Zeng and D. Zhang, "Recent progress in alkaline water electrolysis for hydrogen production and applications," *Prog. Energy Combust. Sci.*, vol. 36, no. 3, pp. 307–326, 2010, doi: 10.1016/j.pecs.2009.11.002.

[6] T. Larsson and S. Skogestad, "Plantwide control - a review and a new design procedure," *Model. Identif. Control*, vol. 21, no. 4, pp. 209–240, 2000, doi: 10.4173/mic.2000.4.2.

[7] S. Kubo *et al.*, "A demonstration study on a closed-cycle hydrogen production by the thermochemical water-splitting iodine - Sulfur process," *Nucl. Eng. Des.*, vol. 233, no. 1–3, pp. 347–354, 2004, doi: 10.1016/j.nucengdes.2004.08.025.

[8] B. Guo and J. Yu, "Model Adaptive Control Based on a Compound Orthogonal Neural Network," *J. Inf. Technol.*, vol. 12, no. 5, pp. 99–107, 2006.

[9] N. Sakaba *et al.*, "Hydrogen production by thermochemical water-splitting IS process utilizing heat from high-temperature reactor HTTR," *Whec 16*, no. June, pp. 1–11, 2006.

[10] B. J. Lee, H. C. No, H. J. Yoon, H. G. Jin, Y. S. Kim, and J. I. Lee, "Development of a flowsheet for iodine-sulfur thermo-chemical cycle based on optimized Bunsen reaction," *Int. J. Hydrogen Energy*, vol. 34, no. 5, pp. 2133–2143, 2009, doi: 10.1016/j.ijhydene.2009.01.006.

[11] B. J. Lee, H. Cheon NO, H. Joon Yoon, S. Jun Kim, and E. Soo Kim, "An optimal operating window for the Bunsen process in the I-S thermochemical cycle," *Int. J. Hydrogen Energy*, vol. 33, no. 9, pp. 2200–2210, 2008, doi: 10.1016/j.ijhydene.2008.02.045.

[12] R. Moore, P. S. Pickard, E. J. Pharma Jr, M. E. Vernon, F. Gelbard, and R. X. Lenard, "United States Patent: Integrated Boiler, Superheater and Decomposer for Sulfuric Acid Decomposition," vol. 2, no. 12, pp. 19–35, 2011, doi: 10.1145/634067.634234.

[13] S. Skogestad, "Economic Plantwide Control," in *Plantwide Control: Recent Developments and Applications*, First., G. P. Rangaiah and V. Kariwala, Eds. John Wiley and Sons Ltd, 2012, pp. 230–251.

[14] S. Skogestad, "Control structure design for complete chemical plants," *Comput. Chem. Eng.*, vol. 28, no. 1–2, pp. 219–234, 2004, doi: 10.1016/j.compchemeng.2003.08.002.

[15] S. Skogestad, "Plantwide control: The search for the self-optimizing control structure," *J. Process Control*, vol. 10, no. 5, pp. 487–507, 2000, doi: 10.1016/S0959-1524(00)00023-8.

[16] J. Nandong, S. Yudi, and T. Moses O, "Novel PCA-Based Technique for Identification of Dominant Variables for Partial Control," *Chem. Prod. Process Model.*, vol. 5, no. 7, 2010.

[17] Q. Zhu *et al.*, "Kinetic and thermodynamic studies of the Bunsen reaction in the sulfur-iodine

thermochemical process," *Int. J. Hydrogen Energy*, vol. 38, no. 21, pp. 8617–8624, 2013, doi: 10.1016/j.ijhydene.2013.04.110.

[18] N. Mohd, "Plantwide Control and Simulation of Sulfur-Iodine Thermochemical Cycle for Hydrogen Production," Curtin University Malaysia, 2018.

[19] W. L. Luyben, "Snowball effects in reactor/separator processes with recycle," *Ind. Eng. Chem. Res.*, vol. 33, pp. 299–305, 1994.

[20] S. Z. Saw, J. Nandong, and U. K. Ghosh, "Optimization of steady-state and dynamic performances of water–gas shift reaction in membrane reactor," *Chem. Eng. Res. Des.*, vol. 134, pp. 36–51, 2018, doi: 10.1016/j.cherd.2018.03.045.

[21] R. Perret, "Solar Thermochemical Hydrogen Production Research (STCH) Thermochemical Cycle Selection and Investment Priority," no. May, 2011.

[22] R. Liberatore, M. Lanchi, A. Giaconia, and P. Tarquini, "Energy and economic assessment of an industrial plant for the hydrogen production by water-splitting through the sulfur-iodine thermochemical cycle powered by concentrated solar energy," *Int. J. Hydrogen Energy*, vol. 37, no. 12, pp. 9550–9565, 2012, doi: 10.1016/j.ijhydene.2012.03.088.

[23] N. V. S. . Murthy Konda and G. P. Rangaiah, "Control Degrees of Freedom Analysis for Plantwide Control of Industrial Process," in *Plantwide Control: Recents Development and Applications*, First., G. P. Rangaiah and V. Kariwala, Eds. John Wiley and Sons Ltd, 2012, pp. 22–42.

[24] N. V. S. N. Murthy Konda, G. P. Rangaiah, and P. R. Krishnaswamy, "A simple and effective procedure for control degrees of freedom," *Chem. Eng. Sci.*, vol. 61, no. 4, pp. 1184–1194, 2006, doi: 10.1016/j.ces.2005.08.026.

[25] N. Mohd, "Plantwide Control and Simulation of Sulfur-Iodine Thermochemical Cycle Process," Curtin University Malaysia, 2018.

[26] Gonzalo A. Almeida Pazmiño and Seunghun Jung, "Thermodynamic modeling of sulfuric acid decomposer integrated with 1 MW tubular SOFC stack for sulfur-based thermochemical hydrogen production.," *Energy Convers. Manag.*, vol. 247, 2021.

[27] H. Seki and Y. Naka, "Optimizing control of CSTR/distillation column processes with one material recycle," *Ind. Eng. Chem. Res.*, vol. 47, no. 22, pp. 8741–8753, 2008, doi: 10.1021/ie800183a.